

## Combustion of methane on $\text{CeO}_2\text{--ZrO}_2$ based catalysts

Christine Bozo, Nolven Guilhaume, Edouard Garbowski, Michel Primet\*

LACE-CNRS, UMR 5634, Université Claude Bernard LYON 1, 43 Boulevard du Onze Novembre 1918, 69622 Villeurbanne Cedex, France

### Abstract

$\text{CeO}_2\text{--ZrO}_2$  solid solutions have been prepared by precipitation of the corresponding hydroxides. They were calcined and aged at various temperatures and characterised by X-ray diffraction measurements, BET and TPR measurements as well by their activity in methane combustion. The  $\text{Ce}_{0.67}\text{Zr}_{0.33}\text{O}_2$  solid exhibited the best thermal stability, the highest oxygen mobility and the best catalytic activity after ageing at  $1000^\circ\text{C}$ . It has been used to support active phases like platinum and manganese oxide.

The fresh  $\text{Pt/Ce}_{0.67}\text{Zr}_{0.33}\text{O}_2$  catalyst was much more active than the corresponding  $\text{Pt/Al}_2\text{O}_3$  solid although a deactivation on stream was observed in the  $200\text{--}500^\circ\text{C}$  temperature range. Nevertheless, the promoting effect of the  $\text{Ce}_{0.67}\text{Zr}_{0.33}$  support disappeared after ageing at  $1000^\circ\text{C}$ .

In the case of  $\text{MnO}_x$  supported onto the  $\text{Ce}_{0.67}\text{Zr}_{0.33}\text{O}_2$  solid solution the activity of the fresh solid is similar to that of the  $\text{MnO}_x/\text{Al}_2\text{O}_3$  catalyst. After ageing at  $1000^\circ\text{C}$ , the solid solution is decomposed, the BET area dramatically decreased and the catalytic properties almost disappeared.

As far as temperature applications exceeding  $1000^\circ\text{C}$  are concerned, the  $\text{CeO}_2\text{--ZrO}_2$  solid solutions are not suitable supports for the catalytic combustion of methane. © 2000 Elsevier Science B.V. All rights reserved.

**Keywords:** Catalytic combustion; Ceria–zirconia solid solutions; Natural gas; Platinum; Manganese oxide; Ageing

### 1. Introduction

Catalytic combustion of methane and other hydrocarbons is a promising new technology for the production of energy without the formation of pollutants like nitrogen oxides [1,2]. For applications in gas turbines and boilers there is an urgent need for the development of new and thermostable catalysts for the combustion of natural gas. A new family of catalysts based on barium hexa-aluminates has recently received considerable attention for application in gas turbines [3–6].

In the case of three-way automotive catalysts,  $\text{CeO}_2$  was widely used and its main function was to act as an oxygen storage component. Neverthe-

less its thermal stability seems to be not sufficient for temperatures exceeding  $1000^\circ\text{C}$ . Several attempts have been performed for the stabilisation of ceria against thermal sintering. Zr appears to be the best additive to increase the resistance of ceria to sintering [7–9]. In addition, the introduction of zirconia into ceria leads to the formation of solid solutions which exhibited to an improvement in the oxygen storage capacity as well as the oxygen mobility [10].

Because of their thermal stability as well as their oxygen mobility  $\text{CeO}_2\text{--ZrO}_2$  solid solutions appear as promising candidates to be used as support (or active phases) in the catalytic combustion of hydrocarbons. Only a limited number of papers have been concerned by this objective [11–13].

In this paper, the stability of  $\text{CeO}_2\text{--ZrO}_2$  solid solutions having various compositions is investi-

\* Corresponding author. Tel.: +33-4-72-44-83-33;  
fax: +33-4-72-44-81-14.  
E-mail address: michel.primet@univ-lyon1.fr (M. Primet)

gated, physicochemical characterisations were also performed at various stages of ageing. In a second step a solid solution was used as support for a noble metal (Pt) and for a transition metal oxide ( $\text{MnO}_x$ ). The catalytic properties of such catalysts have been measured in fresh and aged states in relation with the physicochemical properties of the catalytic material.

## 2. Experimental

### 2.1. Synthesis of the solid solutions

The  $\text{CeO}_2$ – $\text{ZrO}_2$  mixed oxides have been prepared by coprecipitation with ammonia of an aqueous solution containing the corresponding nitrates  $\text{Ce}(\text{NO}_3)_3$ ,  $6\text{H}_2\text{O}$  and  $\text{ZrO}(\text{NO}_3)_2$ ,  $7\text{H}_2\text{O}$  according to the procedure used by Leitenburg et al. [11]. Pure ceria and zirconia have also been prepared as reference supports using the same process. For this purpose an aqueous solution containing the Ce and Zr salts (0.2 M) was prepared and added dropwise to a large excess of ammonia in aqueous solution. The obtained hydroxides were washed and dried at  $100^\circ\text{C}$  for 12 h.

The mixture of the corresponding hydroxides was then calcined under flowing air for 6 h at 500, 700 and  $900^\circ\text{C}$ . The solids calcined at  $700^\circ\text{C}$  were called “fresh samples”.

A simulation for the ageing of a combustion catalyst was performed by treating the “fresh” solid solutions under oxygen (5 vol.%) + water (10 vol.%) in nitrogen for 24 h at  $1000^\circ\text{C}$  and in some cases at  $1200^\circ\text{C}$ . Such a treatment is expected to appreciate the thermal stability of the various solid solutions and to determine the best support for high temperature applications. The solids treated at  $1000^\circ\text{C}$  under  $\text{O}_2 + \text{H}_2\text{O}$  were called “aged samples”.

### 2.2. Elaboration of the catalysts

*Pt supported catalyst.* The selected solid solution, previously calcined at  $700^\circ\text{C}$  under air, was impregnated by an aqueous solution of the Pt precursor free of chloride ions in order to have a Pt content close to 2 wt.%. The  $\text{Pt}(\text{NH}_3)_4(\text{NO}_3)_2$  complex was chosen as Pt precursor. Metallic platinum was formed in two steps (i) decomposition of the ammino complex by

slow heating under oxygen at  $400^\circ\text{C}$ , (ii) reduction under flowing hydrogen at  $300^\circ\text{C}$ . Chemical analysis gave a platinum content of 1.6 wt.%. The “fresh catalyst” was obtained after hydrogen reduction at  $300^\circ\text{C}$  whereas the “aged catalyst” was formed by ageing the fresh one under  $\text{N}_2 + \text{O}_2 + \text{H}_2\text{O}$  at  $1000^\circ\text{C}$  for 24 h.

*Mn supported catalyst.* The same solid solution was also used for supporting Mn oxide. Mn impregnation was carried out by incipient wetness method using a solution of  $\text{Mn}(\text{NO}_3)_2$ ,  $4\text{H}_2\text{O}$ . After an overnight drying at  $100^\circ\text{C}$ , manganese oxide was formed by calcination under air at  $500^\circ\text{C}$  for 6 h. The Mn content deduced from chemical analysis is equal to 7.05 wt.%. A calcination under air at  $500^\circ\text{C}$  led to the fresh catalyst, the treatment of the fresh sample under the ageing mixture at  $1000^\circ\text{C}$  for 24 h led to the “aged catalyst”.

### 2.3. Physicochemical characterisations

Chemical analysis of the various elements (Zr, Ce, Pt, Mn) was performed by AAS after dissolution of the solids in a mixture of concentrated acids ( $\text{HF} + \text{HCl} + \text{HNO}_3$ ).

X-ray diffraction patterns were recorded with a Siemens D500 diffractometer using the  $\text{Cu K}\alpha_1$  line at 0.15406 nm. Spectra were recorded between  $5^\circ$  and  $70^\circ$  ( $2\theta$ ) with a scan rate of  $1.2^\circ \text{min}^{-1}$ . Metallic tungsten powder (60 mesh, 5 wt.%) was added to the solids for an internal calibration. The phases were identified by comparison with the ICDD files.

BET areas were measured by nitrogen adsorption at 77 K using the multipoint method. Before the BET measurement, the samples were evacuated at  $400^\circ\text{C}$  ( $10^{-5}$  Torr) for 2 h.

The fraction of platinum metallic area (or dispersion) was determined by volumetric hydrogen adsorption at room temperature. The Pt supported catalyst is reduced under hydrogen at  $300^\circ\text{C}$  for several hours in the chemisorption cell. It was then treated under vacuum at the same temperature. Isotherm of hydrogen adsorption at room temperature was extrapolated to zero pressure and hydrogen reversibly adsorbed was deduced from a back sorption experiment.

Temperature programmed reduction (TPR) of the solid solutions as well as of the catalysts was performed under a 1 vol.%  $\text{H}_2$  in argon mixture with a

temperature ramp of  $20^{\circ}\text{C min}^{-1}$  from room temperature up to  $1000^{\circ}\text{C}$ . The temperature was maintained at  $1000^{\circ}\text{C}$  for 1 h. Hydrogen consumption was monitored by on-line TCD detector. Prior to the TPR experiment, 150–200 mg of sample were pretreated at  $400^{\circ}\text{C}$  under air for 1 h, then purged under Ar at the same temperature for another 1 h and finally cooled to room temperature. The ( $\text{Ar}+\text{H}_2$ ) mixture was introduced at  $25^{\circ}\text{C}$  onto the previous sample, the hydrogen consumption at  $25^{\circ}\text{C}$  was measured. Only after the recovering of the baseline, the temperature was increased up to  $1000^{\circ}\text{C}$  with the  $20^{\circ}\text{C min}^{-1}$  ramp. When the temperature of  $1000^{\circ}\text{C}$  was reached, the catalyst was maintained under the ( $\text{Ar}+\text{H}_2$  mixture) at  $1000^{\circ}\text{C}$  for additional 1 h in isothermal conditions.

#### 2.4. Catalytic activity measurements

The activity of fresh and aged solid solutions and catalysts for methane combustion was measured on 500 mg of sample in a microreactor. Prior to any catalytic activity measurement, the samples were treated as follows:

1. the supports as well as the Mn supported catalyst were calcined under flowing oxygen at  $400^{\circ}\text{C}$  for 1 h,
2. the Pt supported catalyst was reduced under hydrogen at  $300^{\circ}\text{C}$  for 1 h.

The samples were then cooled under nitrogen to  $250\text{--}350^{\circ}\text{C}$  and the feed of reactants was admitted onto the catalysts. It consists of 1 vol.%  $\text{CH}_4$ , 4 vol.%  $\text{O}_2$  diluted in nitrogen with a flow rate of  $6.4\text{ l h}^{-1}$ , the GHSV is close to  $20\,000\text{ h}^{-1}$ . The activity is measured for 3 h at a given temperature, the reaction temperature was increased by steps of  $50^{\circ}\text{C}$ .

### 3. Results and discussion

#### 3.1. $\text{CeO}_2\text{--ZrO}_2$ solid solutions

Ceria, zirconia and three solid solutions have been prepared with the procedure described in the experimental part [11]. According to the chemical analysis, the solid solutions have the following compositions  $\text{Ce}_{0.83}\text{Zr}_{0.17}\text{O}_2$  (called 83/17),  $\text{Ce}_{0.67}\text{Zr}_{0.33}\text{O}_2$  (called 67/33) and  $\text{Ce}_{0.47}\text{Zr}_{0.53}\text{O}_2$  (called 47/53).

Table 1

BET area ( $\text{m}^2\text{ g}^{-1}$ ) and unit cell parameters ( $\text{\AA}$ ) for the various supports as a function of the calcination temperature and for the two ageing procedures

	$\text{CeO}_2$	83/17	67/33	47/53	$\text{ZrO}_2$
Calcination temperature					
500°C	80	85	104	97	110
700°C	49	58	70	62	57
900°C					
BET	14	27	25	19	31
<i>a</i> parameter	5.416	5.394	5.373		
Aged at $1000^{\circ}\text{C}$	1	3	8	3	8
Aged at $1200^{\circ}\text{C}$	–	–	<1	–	–

The X-ray spectra of  $\text{CeO}_2$  modified by the incorporation of  $\text{Zr}^{4+}$  ions into the lattice were observed for the first calcination temperature, i.e.,  $500^{\circ}\text{C}$ . By increasing the calcination temperature up to  $900^{\circ}\text{C}$ , the peaks did not shift and the half width of the peaks decreased suggesting an increase in the particles' diameter without any phase or composition change. Ceria as well as the 83/17, 67/33 and 60/40 solid solutions are characterised by a face centered cubic cell whereas zirconia and the 47/53 solid solution crystallised in the monoclinic lattice. Neither phase due to pure ceria nor pure zirconia have been observed in the XRD spectra of the solid solutions. The unit cell parameters were given in Table 1 for the various samples after treatment under air at  $900^{\circ}\text{C}$ . A linear decrease of the *a* parameter is observed by introduction of increasing amounts of zirconium into ceria until 40 mol% Zr. Such a decrease was already observed in previous studies [14–16], and it was assigned to the lower ionic radius of  $\text{Zr}^{4+}$  ( $0.84\text{ \AA}$ ) compared to that of  $\text{Ce}^{4+}$  ( $0.97\text{ \AA}$ ) [17]. After ageing at  $1000^{\circ}\text{C}$ , the diffraction peaks became asymmetrical suggesting the formation of new crystallographic phases. The phenomenon was more pronounced after ageing at  $1200^{\circ}\text{C}$  since the new phases are clearly identified by extra lines. Except the 83/17 solid solution the other mixed oxides decompose in two phases after ageing at  $1200^{\circ}\text{C}$ , one phase rich in ceria and identified as  $\text{Ce}_{0.75}\text{Zr}_{0.25}\text{O}_2$ , the other one rich in zirconia and identified as  $\text{Ce}_{0.16}\text{Zr}_{0.84}\text{O}_2$ . The thermal stability of the  $\text{CeO}_2\text{--ZrO}_2$  mixed oxides has been studied after ageing at temperatures between 1000 and  $1400^{\circ}\text{C}$  and the phase diagram indicate that tetragonal  $\text{ZrO}_2$ -rich phase and cubic  $\text{CeO}_2$ -rich phase are thermodynamically stable.

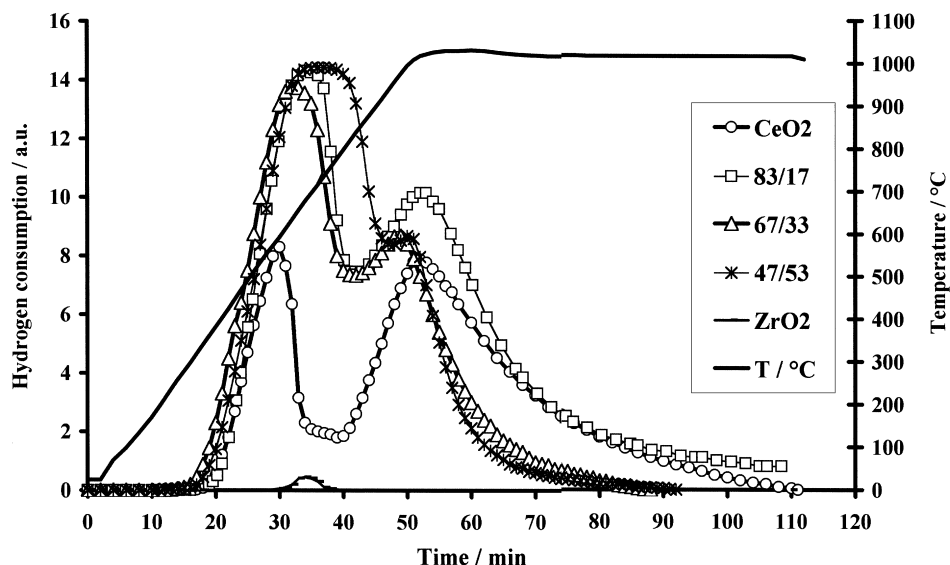


Fig. 1. TPR measurements. Hydrogen consumption as a function of the temperature for  $\text{CeO}_2$  and the various  $\text{CeO}_2$ – $\text{ZrO}_2$  solid solutions after calcination under air at  $700^\circ\text{C}$ .

cally stable phases at these temperatures [18,19]. At  $1200^\circ\text{C}$  it has been found that the limits of the solubility of monoclinic and cubic solid solutions in mol%  $\text{CeO}_2$  are 16 and 80%, respectively. Thus the ageing of the  $\text{Ce}_{0.67}\text{Zr}_{0.33}\text{O}_2$  and  $\text{Ce}_{0.47}\text{Zr}_{0.53}\text{O}_2$  mixed oxides leads to the two most stable solid solutions according to thermodynamics [18].

Table 1 shows the evolution of the BET area of the supports for different temperatures of calcination and for the two ageing procedures. Among the three solid solutions, the 67/33 composition presents the largest BET area values. In addition such a solid has the best resistance to a thermal ageing performed at  $1000^\circ\text{C}$ . However after ageing at  $1200^\circ\text{C}$ , a drastic loss in the BET area was observed and only ageing performed at  $1000^\circ\text{C}$  was considered in the following parts.

The TPR profiles of the fresh supports are shown in Fig. 1. Zirconia is almost unreducible by hydrogen at  $1000^\circ\text{C}$ . By contrast the other samples present two peaks of reduction. In the case of ceria the first peak (at  $583^\circ\text{C}$ ) is attributed to the reduction of the surface and the second one (at ca.  $950^\circ\text{C}$ ) to the reduction of the bulk [20]. In the case of the solid solutions, the first peak corresponds to the reduction of the surface as well as that of some subsurface layers [8,16,21]: reduction at the surface and in the bulk occur at the same time. By using the correlation previously established by Perrichon et al. [22] (the reduction of  $1\text{ m}^2$  of ceria requires  $3.9\text{ }\mu\text{mol H}_2$ ) [22], it is possible to determine the number of layers which have been reduced under the first peak of hydrogen consumption after taking into account the ceria content of the solid

Table 2

TPR measurements. Amounts of hydrogen consumption and number of reduced layers in the first peak of reduction<sup>a</sup>

Sample	BET area ( $\text{m}^2\text{ g}^{-1}$ )	Temperature first TPR peak ( $^\circ\text{C}$ )	Catalyst ( $\mu\text{mol H}_2\text{ g}^{-1}$ )	No. of reduced layers
$\text{CeO}_2$	49	583	198	1.0
83/17	58	668	541	2.74
67/33 fresh	70	679	830	4.1
67/33 aged at $1000^\circ\text{C}$	8	770	694	29.9
47/53	62	740	927	7.0

<sup>a</sup>Samples pretreated at  $700^\circ\text{C}$  under air.

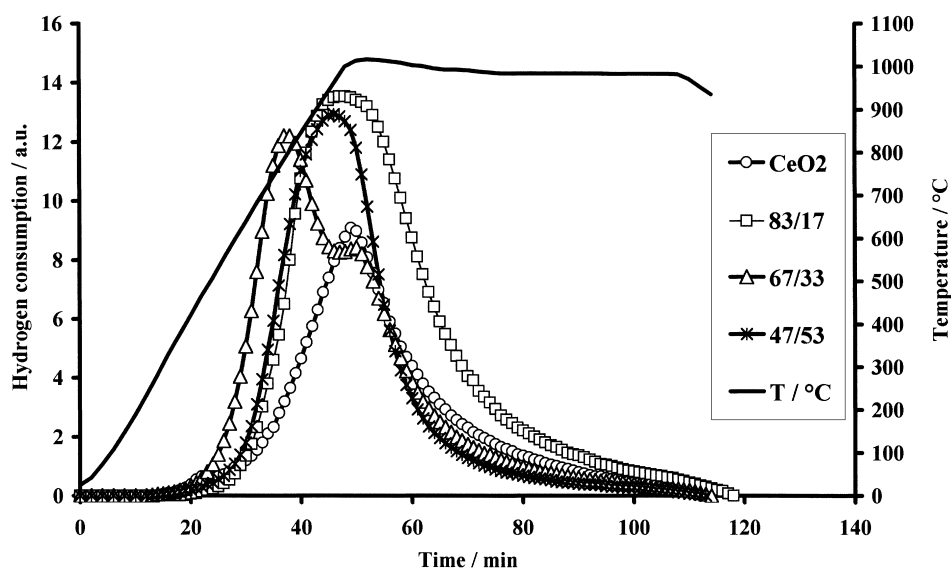


Fig. 2. TPR measurements. Hydrogen consumption as a function of the temperature for  $\text{CeO}_2$  and the various  $\text{CeO}_2\text{--ZrO}_2$  solid solutions after ageing at  $1000^\circ\text{C}$  under  $\text{O}_2\text{+H}_2\text{O}$  in nitrogen.

solution. These values are given in Table 2. They show that the reducibility of the solid solution increases with the amount of incorporated zirconium [23].

After ageing at  $1000^\circ\text{C}$ , the TPR profiles are strongly modified (Fig. 2). Excepting for the 67/33 solid, the low temperature peak disappeared from the TPR traces after ageing. In the case of the 67/33 solid, the number of layers reduced in the first peak increased until ca. 29 layers. Such a result suggests a higher mobility of oxygen surface and subsurface species after ageing at high temperature. The participation of O from the bulk of very low surface area ceria–zirconia mixed oxides has been also evidenced in oxygen storage capacity measurements [10,24,25].

Finally the catalytic activity of the ceria as well as that of the  $\text{CeO}_2\text{--ZrO}_2$  solid solutions was measured in the fresh and aged states. The results are shown in Fig. 3a and b. Fresh samples exhibit a non-negligible catalytic activity with a temperature of half conversion ( $T_{50}$ ) varying from  $572^\circ\text{C}$  for  $\text{CeO}_2$  to  $593^\circ\text{C}$  for the 47/73 sample. As previously observed for the catalytic oxidation of isobutane (10), the introduction of  $\text{Zr}^{4+}$  ions in the  $\text{CeO}_2$  lattice does not markedly affect the catalytic activity. Ageing at  $1000^\circ\text{C}$  considerably decreased the catalytic activity, the  $T_{50}$  temperatures largely exceed  $700^\circ\text{C}$ . Nevertheless, and as for the

TPR measurements, the less deactivated solid solution corresponds to the 67/33 composition.

In conclusion, the  $\text{Ce}_{0.67}\text{Zr}_{0.33}\text{O}_2$  solid solution was chosen for supporting active phases in  $\text{CH}_4$  combustion like metallic platinum and manganese oxides. This support was selected because of its specific properties after ageing at  $1000^\circ\text{C}$ : relatively high BET area, preservation of oxygen mobility and own catalytic properties in methane combustion.

### 3.2. $\text{Pt/Ce}_{0.67}\text{Zr}_{0.33}\text{O}_2$ catalyst

Table 3 gives the main characteristics of the catalysts in fresh and aged states. The BET areas are not changed in both states by the presence of platinum. The X-ray pattern of the catalyst is similar to that of the solid solution in the fresh state, Pt particles were not detected. After ageing at  $1000^\circ\text{C}$ , the crystallographic phases of the solid solution are not modified whereas Pt is now detected by a peak at  $2\theta=39.7^\circ$ . The fraction of exposed platinum was deduced from chemisorption experiments, it was equal to 40% in the fresh state, which corresponds to a mean Pt particles, dimension of 2.5 nm. In the aged state the amount of chemisorbed hydrogen is below the detection limit of the apparatus: a drastic sintering of the Pt particles

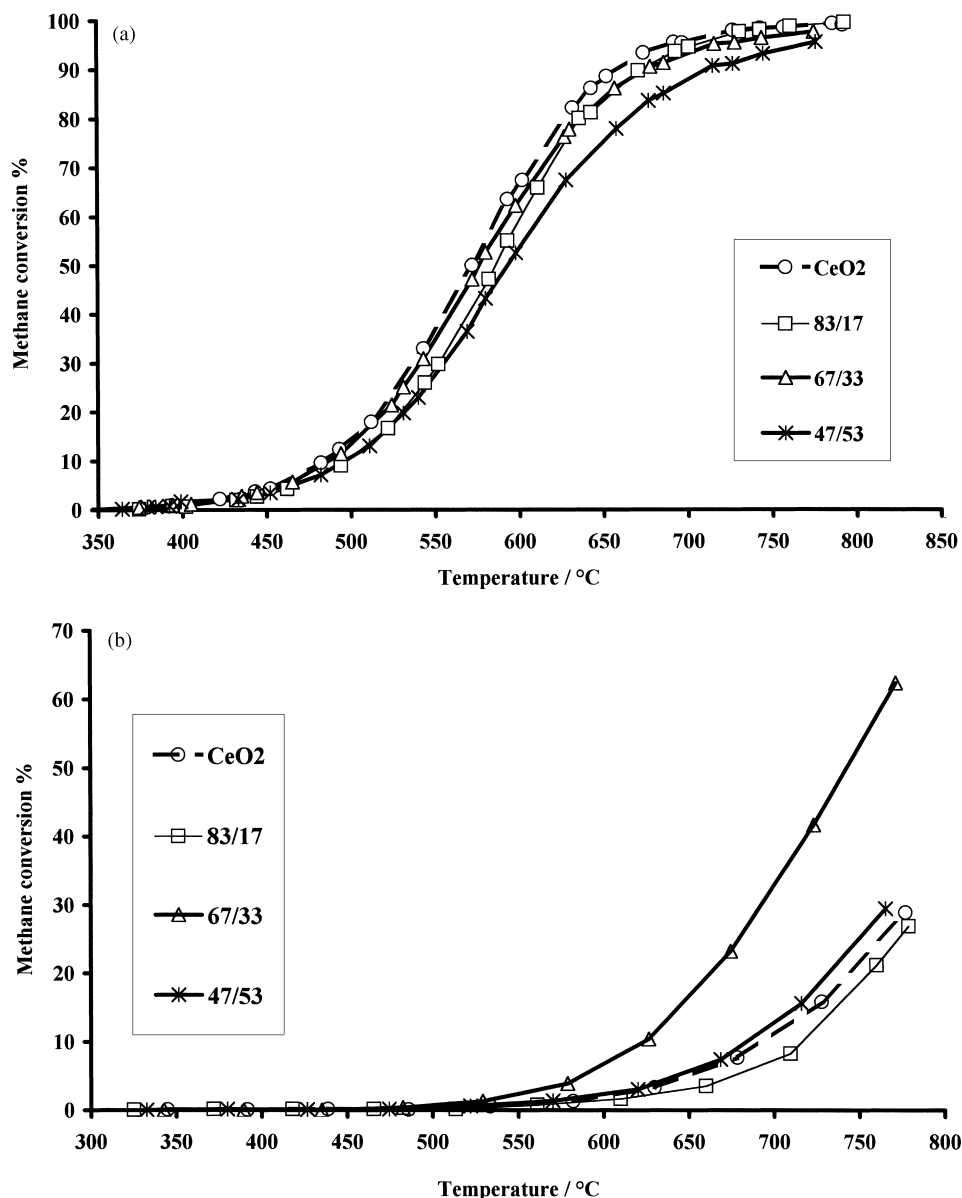


Fig. 3. Catalytic activity in the complete oxidation of methane over CeO<sub>2</sub> and the three CeO<sub>2</sub>–ZrO<sub>2</sub> solid solutions: (a) fresh samples, calcination under air at 700°C, and (b) aged samples, calcination at 1000°C under O<sub>2</sub>+H<sub>2</sub>O in nitrogen.

and/or their encapsulation by the CeO<sub>2</sub>–ZrO<sub>2</sub> support may be expected upon ageing [24,25].

The TPR profiles of the fresh and aged Pt/Ce<sub>0.67</sub>Zr<sub>0.33</sub>O<sub>2</sub> catalyst are shown in Fig. 4. In the case of the fresh catalyst, a large amount of hydrogen is consumed at room temperature (not shown in the figure). During

the heating ramp, the TPR profile shows three peaks at 147, 565 and 1000°C. By comparison with the TPR trace of the support alone, it can be concluded that the presence of Pt led to a shift of the peak at 679°C to lower temperatures (147 and 565°C). The hydrogen consumption at 25°C is equal to 419  $\mu\text{mol g}^{-1}$

Table 3

Main characteristics of the Pt/Ce<sub>0.67</sub>Zr<sub>0.33</sub>O<sub>2</sub> catalyst in the fresh state and after ageing at 1000°C

Property	Fresh catalyst	Aged catalyst
BET area	69 m <sup>2</sup> g <sup>-1</sup>	7 m <sup>2</sup> g <sup>-1</sup>
Fraction of accessible Pt	40%	<1%
H <sub>2</sub> consumption at 25°C	419 μmol g <sup>-1</sup> , 1.6–1.9 layers	0
T <sub>50</sub>	335°C	620°C
E <sub>act</sub>	75 kJ mol <sup>-1</sup>	106 kJ mol <sup>-1</sup>

catalyst. It corresponds to the reduction of platinum, supposed to be in the form of PtO, as well as to the reduction of a fraction of the support. According to the hypothesis adopted for the reduction of platinum (reduction of Pts–O species or reduction of the bulk platinum oxide), the reduction of the solid solution at 25°C is between 1.6 and 1.9 layer. In the case of the solid solution free of platinum, the first peak of surface reduction was observed at ca. 680°C. Since in the case of Pt/Ce<sub>0.67</sub>Zr<sub>0.33</sub>O<sub>2</sub> catalyst such a reduction occurs at room temperature, it may be concluded that the addition of platinum on the solid solution strongly enhances the mobility of surface and sublayer oxygen

species. In a similar way, for Rh-loaded CeO<sub>2</sub>–ZrO<sub>2</sub> solid solutions, the addition of ZrO<sub>2</sub> lowers the temperature of the reduction of bulk Ce<sup>4+</sup> ions by ca. 500°C [23].

In the case of the aged Pt/Ce<sub>0.67</sub>Zr<sub>0.33</sub>O<sub>2</sub> catalyst, the TPR curve was strongly modified (Fig. 4). No hydrogen consumption was detected at room temperature. Two peaks of reduction were observed at 306 and 1000°C. Since the accessible metallic fraction of the Pt particles is very low, the peak at 306°C (258 μmol H<sub>2</sub> g<sup>-1</sup> catalyst) is only attributed to the reduction of the first layers of the 67/33 solid solution, 12.4 layers are reduced at this temperature. As in the case of the ceria–zirconia solid solution free of Pt, bulk oxygen species are more involved in the aged catalyst in comparison with the fresh one. The peak at 306°C observed in presence of Pt probably results from the shift noted at 770°C in the case of the aged 67/33 solid solution. Here also the oxygen mobility of the support is enhanced by Pt addition although the metallic phase was very poorly dispersed.

The catalytic activity of the Pt/Ce<sub>0.67</sub>Zr<sub>0.33</sub>O<sub>2</sub> catalyst is given in Fig. 5 for the fresh and the aged states, for comparison purpose the activities of the support in the fresh and the aged states are also included. The

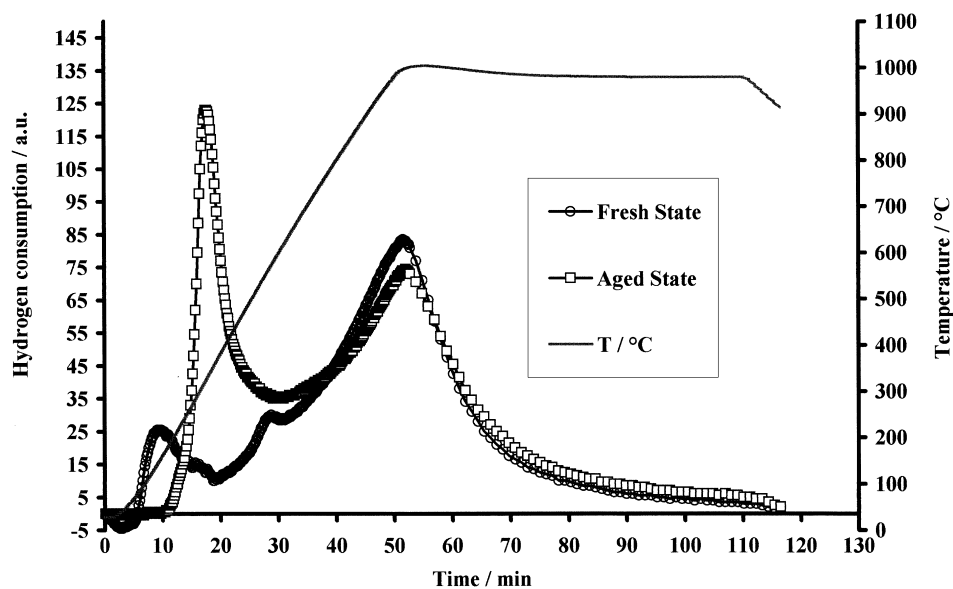


Fig. 4. TPR measurements. Hydrogen consumption as a function of the temperature for the fresh and aged Pt/Ce<sub>0.67</sub>Zr<sub>0.33</sub>O<sub>2</sub> catalyst. Ageing was performed at 1000°C under O<sub>2</sub>+H<sub>2</sub>O in nitrogen.

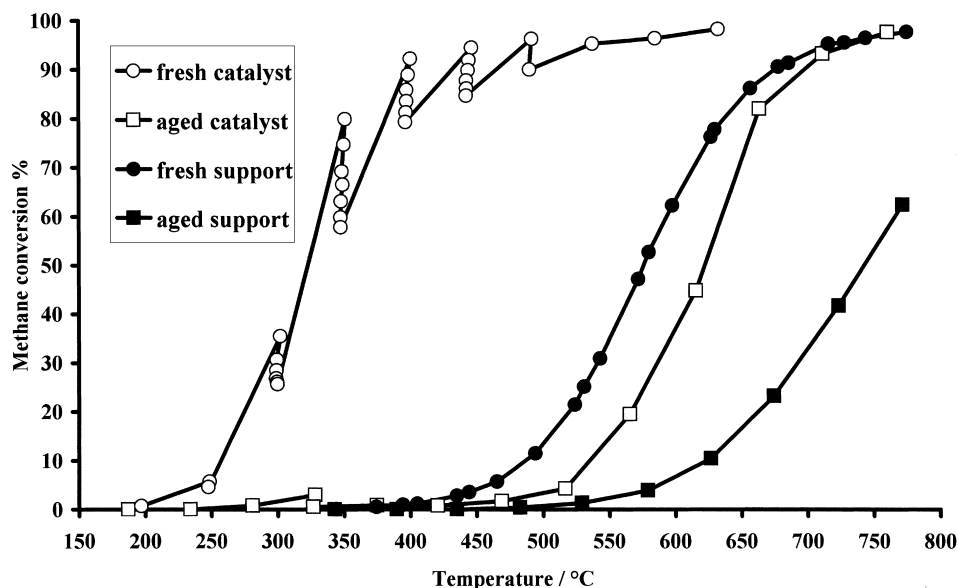


Fig. 5. Conversion of  $\text{CH}_4$  into  $\text{CO}_2$  as a function of the temperature for the  $\text{Pt/Ce}_{0.67}\text{Zr}_{0.33}\text{O}_2$  catalyst as well as for the  $\text{Ce}_{0.67}\text{Zr}_{0.33}\text{O}_2$  in fresh and aged states.

activity of the fresh sample is strongly enhanced in comparison with the support alone, the  $T_{50}$  decreased from 576 to 335 °C after Pt deposition. This catalyst is even more active than the corresponding one us-

ing  $\text{Al}_2\text{O}_3$  as support ( $T_{50}=470^\circ\text{C}$ ) [27] whereas its activity is comparable to that of a  $\text{Pd/Al}_2\text{O}_3$  catalyst ( $T_{50}=320^\circ\text{C}$ ) [28,30]. Fig. 6 compares the activity of  $\text{Pt/Al}_2\text{O}_3$  and  $\text{Pt/Ce}_{0.67}\text{Zr}_{0.33}\text{O}_2$  catalysts as a func-

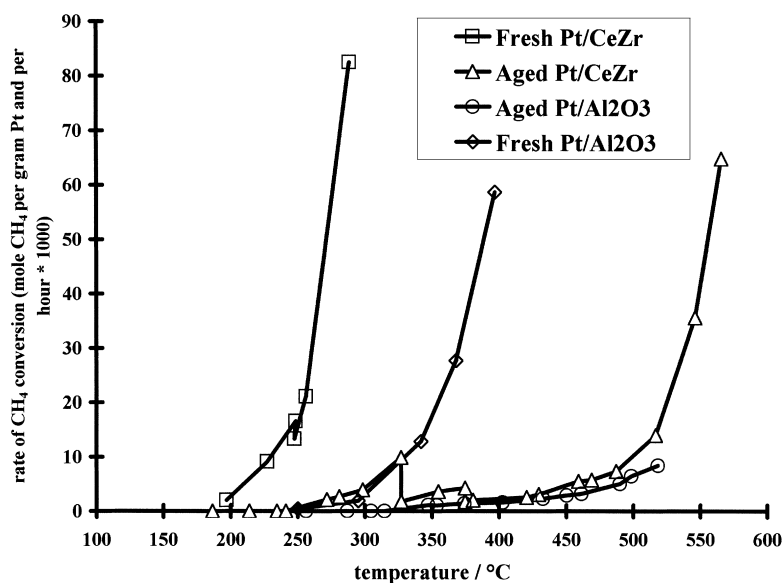


Fig. 6. Catalytic activity in methane combustion for platinum supported on alumina and on the  $\text{Ce}_{0.67}\text{Zr}_{0.33}\text{O}_2$  solid solution in fresh and aged states.



tion of the temperature. As far as the fresh states are concerned, it is quite clear that the solid solution leads to an improvement of the catalytic activity. In accordance with our TPR results, the mobility of surface oxygen species of the support is enhanced by the presence of Pt particles leading to a large improvement of the catalytic performances.

In the 300–450°C range, the conversion decreases with the time on stream at a given temperature. This behaviour is illustrated by Fig. 7 in which the conversion of CH<sub>4</sub> into CO<sub>2</sub> at 350°C was plotted as a function of the reaction time. After a reaction time of 12 h a loss of conversion from 80 to 40% was observed. The activity was fully regenerated by treating the deactivated sample under hydrogen at 300°C for 1 h (Fig. 7). On the contrary, the deactivated catalyst did not recover its activity by treatment under nitrogen or oxygen at 350 or 500°C (Fig. 7). Such a behaviour is typical for Pt support on a CeO<sub>2</sub>–ZrO<sub>2</sub> solid solution, the deactivation involved probably active sites of the support. Different causes of deactivation may be considered:

- poisoning by water and/or CO<sub>2</sub>, such an inhibiting effect of CO<sub>2</sub> and/or H<sub>2</sub>O would be suppressed by a treatment at temperature high enough to decompose surface carbonates or to condense hydroxyl groups. Such an hypothesis was ruled out since a treatment

under nitrogen at 500°C does not modify the deactivation whereas CO<sub>3</sub><sup>2-</sup> and OH groups are eliminated. The decomposition of CO<sub>3</sub><sup>2-</sup> groups was followed by in situ FTIR spectroscopy.

- a sintering of the Pt particles could explain the loss of activity. Nevertheless the fraction of exposed platinum atoms in the deactivated state is close to that measured in the fresh state.

The deactivation is probably due to the progressive formation of some oxidised species bonded to the support or/and to the platinum particles, the identification of the species responsible for such a deactivation is still under study.

After ageing at 1000°C, the activity strongly decreased, the *T*<sub>50</sub> temperature increased from 335 to ca. 620°C. The catalytic activity is close to that of Pt/Al<sub>2</sub>O<sub>3</sub> aged in the same conditions (Fig. 6) [28–30]. Even if the right Ce<sub>0.67</sub>Zr<sub>0.33</sub>O<sub>2</sub> solid solution without any demixion is still present and if the BET area value (7 m<sup>2</sup> g<sup>-1</sup>) is not too low, the beneficial effect of the solid solution onto the catalytic properties of Pt in methane combustion is completely suppressed for the Pt/Ce<sub>0.67</sub>Zr<sub>0.33</sub>O<sub>2</sub> solid aged at 1000°C. An encapsulation of the metal particles has been considered, after ageing, in the case of rhodium and platinum deposited onto a CeO<sub>2</sub>–ZrO<sub>2</sub> solid solution [27]. One important parameter in favour of the encapsulation would be the

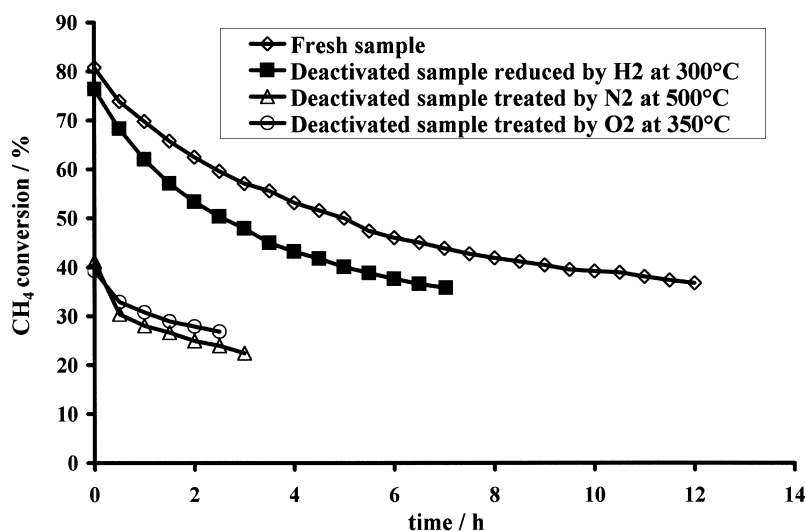


Fig. 7. Methane conversion into CO<sub>2</sub> on the fresh Pt/Ce<sub>0.67</sub>Zr<sub>0.33</sub>O<sub>2</sub> catalyst at 350°C as a function of the time on stream. Activity was measured on fresh catalyst as well as on deactivated catalysts subsequently treated, either under nitrogen, oxygen or hydrogen.

Table 4

Main characteristics of the  $\text{MnO}_x/\text{Ce}_{0.67}\text{Zr}_{0.33}\text{O}_2$  catalyst in the fresh state and after ageing at  $1000^\circ\text{C}$ 

Property	Fresh catalyst	Aged catalyst
BET area	$62\text{ m}^2\text{ g}^{-1}$	$0.4\text{ m}^2\text{ g}^{-1}$
Crystallographic phases	$\text{Ce}_{0.67}\text{Zr}_{0.33}\text{O}_2 + \text{MnO}_2$	$\text{Ce}_{0.75}\text{Zr}_{0.25}\text{O}_2 + \text{Ce}_{0.16}\text{Zr}_{0.84}\text{O}_2 + \text{Mn}_3\text{O}_4$
$T_{50}$	$525^\circ\text{C}$	—
$E_{\text{act}}$	$83\text{ kJ mol}^{-1}$	—

formation of a bulk oxide of the noble metal in the ageing conditions [26]. The formation of Pt bulk oxides which does not occur in similar conditions could be at the origin of the non-encapsulation of the Pt particles [26].

### 3.3. $\text{MnO}_x/\text{Ce}_{0.67}\text{Zr}_{0.33}\text{O}_2$ catalyst

Table 4 gives the main characteristics of this catalyst in the fresh and aged states.

Before ageing, the BET area of the catalyst is similar to that of the support. By contrast, after ageing, the resulting BET area is very low ( $0.4\text{ m}^2\text{ g}^{-1}$ ) and much lower than that of the aged  $\text{Ce}_{0.67}\text{Zr}_{0.33}\text{O}_2$  support ( $8\text{ m}^2\text{ g}^{-1}$ ). For the fresh solid, the phases identified by X-ray analysis are those of the 67/33 solid solution and  $\text{MnO}_2$ . For the aged solid,  $\text{Mn}_3\text{O}_4$  is

detected and a phase segregation of the solid solution is observed: the  $\text{Ce}_{0.75}\text{Zr}_{0.25}\text{O}_2$  and  $\text{Ce}_{0.16}\text{Zr}_{0.84}\text{O}_2$  phases are now detected like in the case of the ageing of the solid solutions at  $1200^\circ\text{C}$  under  $\text{O}_2$  and  $\text{H}_2\text{O}$ . Such a phase segregation might explain the dramatic loss of surface area after ageing.  $\text{MnO}_x$  deposition strongly decreased the thermal stability of the 67/33 solid solution which is decomposed at  $1000^\circ\text{C}$  in the presence of  $\text{MnO}_x$ .

The TPR profiles of the  $\text{MnO}_x/\text{Ce}_{0.67}\text{Zr}_{0.33}\text{O}_2$  catalyst in fresh and aged states are given in Fig. 8. For the fresh catalysts two main peaks are observed, the first one close to  $500^\circ\text{C}$  and the second one at ca.  $900^\circ\text{C}$ . The hydrogen consumption at  $500^\circ\text{C}$  corresponds to the reduction of  $\text{MnO}_x$  and to the first layers of the solid solution (reduction observed at ca.  $680^\circ\text{C}$  in the absence of Mn). By assuming the reduction of  $\text{MnO}_2$

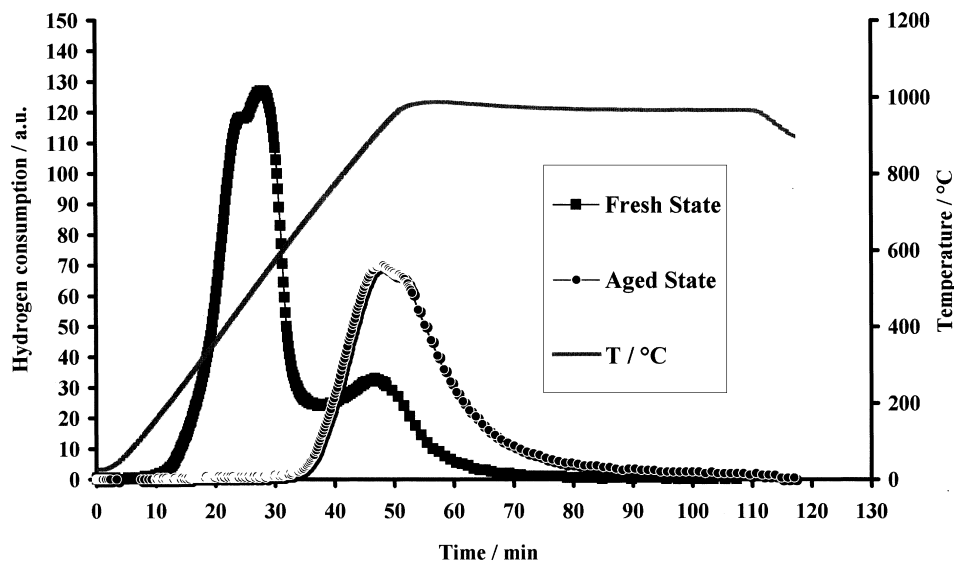


Fig. 8. TPR measurements. Hydrogen consumption as a function of the temperature for the fresh (■) and aged (●)  $\text{MnO}_x/\text{Ce}_{0.67}\text{Zr}_{0.33}\text{O}_2$  catalyst. Ageing was performed at  $1000^\circ\text{C}$  under  $\text{O}_2 + \text{H}_2\text{O}$  in nitrogen.

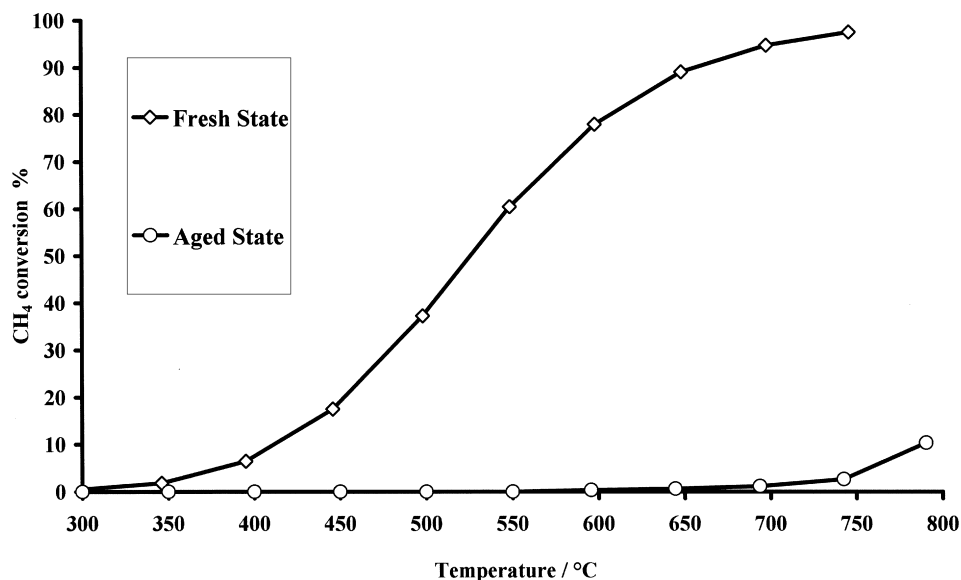


Fig. 9. Catalytic activity in methane combustion for  $\text{MnO}_x$  supported on the  $\text{Ce}_{0.67}\text{Zr}_{0.33}\text{O}_2$  solid in fresh and aged states.

into  $\text{MnO}$  in the first TPR peak, the reduction at  $500^\circ\text{C}$  of the  $\text{Ce}_{0.67}\text{Zr}_{0.33}\text{O}_2$  solid solution concerns 5.0 layers. The aged catalyst exhibited only one peak of reduction at ca.  $950^\circ\text{C}$ .

The catalytic activity of the  $\text{MnO}_x/\text{Ce}_{0.67}\text{Zr}_{0.33}\text{O}_2$  catalyst in the two states is shown in Fig. 9. A comparison with  $\text{MnO}_x/\text{Al}_2\text{O}_3$  is given in Fig. 10 for the same type of ageing. In the fresh state the activ-

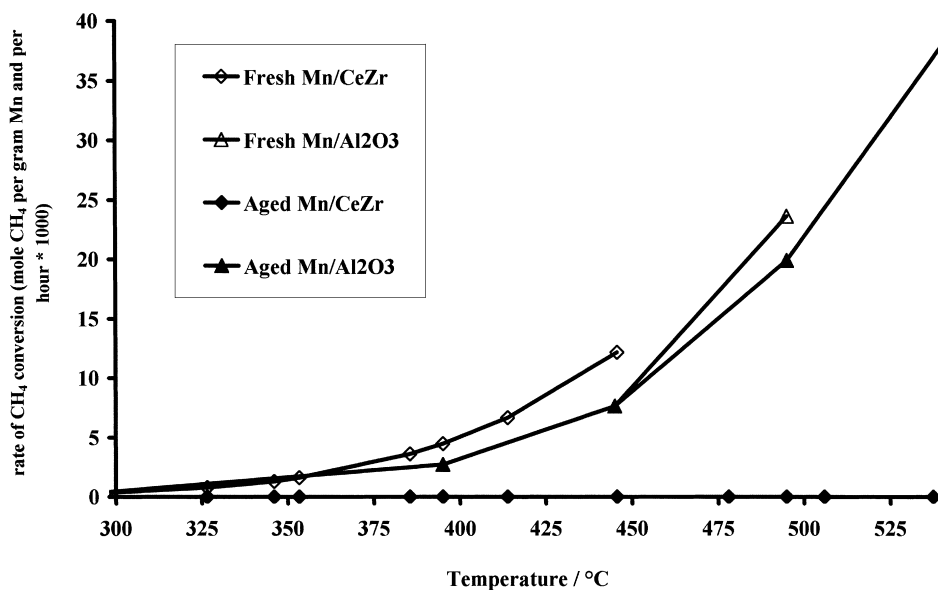


Fig. 10. Comparison of the activities of  $\text{MnO}_x/\text{Al}_2\text{O}_3$  and  $\text{MnO}_x/\text{Ce}_{0.67}\text{Zr}_{0.33}\text{O}_2$  catalysts at low conversion in the fresh and the aged states.

ity Mn oxide supported onto  $\text{Ce}_{0.67}\text{Zr}_{0.33}\text{O}_2$  ( $T_{50}=525^\circ\text{C}$ ) is slightly better than that of the support ( $T_{50}=576^\circ\text{C}$ ). Fig. 10 shows that at low conversion the  $\text{Ce}_{0.67}\text{Zr}_{0.33}\text{O}_2$  solid solution has a slight positive effect on the catalytic activity in the fresh state. Nevertheless, over the full temperature range studied, the promoting effect of the  $\text{Ce}_{0.67}\text{Zr}_{0.33}$  support onto the catalytic activity of manganese oxide is rather small. In addition, the catalytic activity is close to that of the  $\text{Ce}_{0.67}\text{Zr}_{0.33}\text{O}_2$  support. After ageing the catalytic activity almost disappeared since the conversion at  $800^\circ\text{C}$  is ca. 10%, i.e. comparable to the activity due to the homogeneous reaction measured with a reactor filled with silica powder. Such an aged catalyst is largely less active than the corresponding  $\text{MnO}_x/\text{Al}_2\text{O}_3$  solid (Fig. 10). Taking into account the BET areas of the  $\text{Ce}_{0.67}\text{Zr}_{0.33}\text{O}_2$  support and of the  $\text{MnO}_x/\text{Ce}_{0.67}\text{Zr}_{0.33}\text{O}_2$  catalyst, the intrinsic catalytic activity in  $\text{CH}_4$  combustion has been calculated at  $700^\circ\text{C}$ : the intrinsic activity of the catalyst is equal to  $1.7 \times 10^{-4} \text{ mol CH}_4 \text{ h}^{-1} \text{ m}^{-2}$ , whereas the corresponding value for the support is  $2.0 \times 10^{-4} \text{ mol CH}_4 \text{ h}^{-1} \text{ m}^{-2}$ . The proximity of these two values strongly suggests that manganese oxide is no longer present at the surface of the support and is probably encapsulated or dissolved into the solid solution crystallites.

In the case of fresh Mn-doped ceria–zirconia solid solutions, Terribile et al. [13] have found a slight positive effect of Mn addition for the combustion of  $\text{C}_{1+}$  alkanes. For instance, the  $T_{50}$  temperature for  $\text{iC}_4\text{H}_{10}$  combustion decreased by ca.  $60^\circ\text{C}$  after introducing 5 mol% Mn in the  $\text{Ce}_{0.8}\text{Zr}_{0.2}\text{O}_2$  mixed oxide. Such a promoting effect was strongly decreased in methane combustion, like in the present. The authors concluded that low temperature reaction conditions (combustion of  $\text{C}_{1+}$  alkanes) might favour the reactivity of catalysts whose redox behaviour is promoted at low temperature.

In conclusion, the use of the  $\text{Ce}_{0.67}\text{Zr}_{0.33}\text{O}_2$  solid solutions as support of Mn oxide has a limited beneficial effect on the catalytic activity in the fresh state. On the other hand, the aged solid has almost no catalytic activity. Such a behaviour is probably due to the loss of the thermal stability leading to the appearance of new solid solutions associated with a drastic loss of the surface area. In addition, it seems that manganese species are not accessible to the

reactants.  $\text{MnO}_x$  seems to be responsible for the loss of the thermal stability of the solid solution.

#### 4. Conclusion

The thermal stability of several solid solutions  $\text{Ce}_{1-x}\text{Zr}_x\text{O}_2$  has been investigated in the range  $0 < x < 0.53$ . After ageing at  $1000^\circ\text{C}$  under oxygen and steam, the  $\text{Ce}_{0.67}\text{Zr}_{0.33}\text{O}_2$  solid showed the best thermal stability and was selected as support for active phases. It was found that the various solid solutions have a non-negligible catalytic activity in methane combustion.

The  $\text{Pt}/\text{Ce}_{0.67}\text{Zr}_{0.33}\text{O}_2$  catalyst was very active in  $\text{CH}_4$  combustion, its activity was much higher than that of platinum deposited on alumina and comparable to that of a  $\text{Pd}/\text{Al}_2\text{O}_3$  catalyst. Nevertheless, in isothermal conditions a deactivation on stream is observed in the  $200\text{--}500^\circ\text{C}$  temperature range. After ageing at  $1000^\circ\text{C}$  the thermal stability of the  $\text{Ce}_{0.67}\text{Zr}_{0.33}$  solution is preserved, but the activity is similar to that of an aged  $\text{Pt}/\text{Al}_2\text{O}_3$  catalyst: the positive effect of the  $\text{Ce}_{0.67}\text{Zr}_{0.33}\text{O}_2$  support is no longer observed.

The catalyst obtained by supporting manganese oxide onto the  $\text{Ce}_{0.67}\text{Zr}_{0.33}\text{O}_2$  solid solution is slightly more active than the corresponding  $\text{MnO}_x/\text{Al}_2\text{O}_3$  catalyst. After ageing at  $1000^\circ\text{C}$ , the presence of manganese oxide leads to a complete loss of the thermal stability of the solid solution. A segregation of phases is observed with the formation of two new solid solutions,  $\text{Ce}_{0.75}\text{Zr}_{0.25}\text{O}_2$  and  $\text{Ce}_{0.16}\text{Zr}_{0.84}\text{O}_2$ , at the same time the BET area dramatically decreases down to  $0.4 \text{ m}^2 \text{ g}^{-1}$ . The aged sample has no catalytic activity in methane combustion below  $700^\circ\text{C}$ .

For the above results it can be concluded that the  $\text{CeO}_2\text{--ZrO}_2$  solid solutions are not suitable supports for methane catalytic combustion as far as high temperatures applications are concerned.

#### Acknowledgements

The authors fully acknowledge GAZ DE FRANCE (Direction de la Recherche, Département des Etudes Générales, Pôle Combustion Catalytique et Mécanique des Fluides) and ADEME (Agence de l'Environnement et de la Maîtrise de l'Energie) for

financial support as well as for stimulating discussions. They are very grateful to Mr. B. Béguin for his assistance in the catalytic activity measurements.

## References

- [1] NO<sub>x</sub>: basic mechanisms of formation and destruction and their applications to emission control technologies, J.W. Patrick, K.M. Thomas (Eds.), *Fuel* 73 (1994) 1379.
- [2] M.F.M. Zwinkels, S.G. Järås, P.G. Menon, T.A. Griffin, *Catal. Rev.Sci. Eng.* 35 (1990) 319.
- [3] H. Inoue, K. Sekizawa, K. Eguchi, H. Aria, *Catal. Today* 47 (1999) 181.
- [4] B.W.-L. Jang, R.M. Nelson, J.J. Spivey, M. Ocal, R. Oukaci, G. Marcellin, *Catal. Today* 47 (1999) 103.
- [5] G. Groppi, C. Cristiani, P. Forzatti, *J. Catal.* 168 (1997) 95.
- [6] D. Naoufal, J.M. Millet, E. Garbowski, Y. Brullé, M. Primet, *Catal. Lett.* 54 (1998) 141.
- [7] M. Ozawa, M. Kimura, A. Isogai, *J. Alloys Compounds* 193 (1993) 73.
- [8] J.P. Cuif, G. Blanchard, O. Touret, A. Seigneurin, M. Marczi, E. Quemere, *SAE Paper* 961906 (1996).
- [9] P. Fornasiero, G. Balducci, J. Kašpar, S. Meriani, R. di Monte, M. Graiani, *Catal. Today* 29 (1996) 47–52.
- [10] C.E. Hori, H. Permana, R.Y. Simon Ng, A. Brenner, K. More, K.M. Rahmoeller, D. Belton, *Appl. Catal. B* 16 (1998) 105.
- [11] C. de Leitenburg, A. Trovarelli, J. Llorca, F. Cavani, G. Bini, *Appl. Catal. A* 139 (1996) 161.
- [12] E. Bekyarova, P. Fornasiero, J. Kašpar, M. Graziani, *Catal. Today* 45 (1998) 178.
- [13] D. Terribile, A. Trovarelli, C. De Leitenburg, A. Primavera, G. Dolcetti, *Catal. Today* 47 (1999) 133.
- [14] M.H. Yao, R.J. Baird, F.W. Kuntz, T.E. Hoost, *J. Catal.* 166 (1997) 67.
- [15] J.G. Nunan, W.B. Williamson, H.J. Robota, *SAE Paper* 960798 (1996).
- [16] F. Fajardie, Ph. D. Thesis, Paris VI, France, 1996.
- [17] R.D. Shannon, C.T. Prewitt, *Acta Crystallogr. B* 25 (1969) 925.
- [18] E. Tani, M. Yoshimura, S. Somiya, *J. Am. Ceram. Soc.* 66 (1983) 506.
- [19] A.E. McHale, *Phase Diagrams for Ceramists*, Annual 1991, Vol. 20, 1991.
- [20] H.C. Yao, Y.F. Yu Yao, *J. Catal.* 86 (1984) 254.
- [21] P. Fornasiero, G. Balducci, R. di Monte, J. Kašpar, V. Sergo, G. Gubitosa, A. Ferrero, M. Graziani, *J. Catal.* 164 (1996) 173.
- [22] V. Perrichon, A. Laachir, S. Abouardanasse, O. Touret, G. Blanchard, *Appl. Catal. A* 129 (1995) 69.
- [23] P. Fornasiero, R. Di Monte, G. Ranga Rao, J. Kašpar, S. Meriani, A. Trovarelli, M. Graziani, *J. Catal.* 151 (1995) 168.
- [24] G. Ranga Rao, J. Kašpar, S. Meriani, R. Di Monti, M. Graziani, *Catal. Lett.* 24 (1994) 107.
- [25] S. Salasc, Ph.D. Thesis, Lyon, France, November 1998.
- [26] G.W. Graham, H.-W. Jen, W. Chun, R.W. Mc Cabe, *J. Catal.* 182 (1999) 228.
- [27] P. Fornasiero, J. Kašpar, V. Sergo, M. Graziani, *J. Catal.* 182 (1999) 56.
- [28] P. Briot, A. Auroux, D. Jones, M. Primet, *Appl. Catal.* 59 (1990) 141.
- [29] P. Briot, M. Primet, *Appl. Catal.* 68 (1991) 301.
- [30] M. Primet, et al., unpublished results.